Lipid-Glycoadjuvant@AuNPs Inhibits Tumor Gowth and Regulates Tumor Microenvironments by Tumor-Specific CTL-Ferived IFNγ

Xiaojing Xu
Soochow University
Cheng Yi
Soochow University
Youzhen Ge
Soochow University
Tianyun Feng
Soochow University
Mengjie Liu
Soochow University
Cenhao Wu
Soochow University Affiliated No 1 People\'s Hospital: First Affiliated Hospital of Soochow University
Xiang Chen
Yangzhou University
Jun Zou
Soochow University Affiliated No 1 People\'s Hospital: First Affiliated Hospital of Soochow University
Weidong Zhang
Soochow University
Lixiang Zhao (zhaolixiang@suda.edu.cn)
Soochow University

Research

Keywords: lipid-glycoadjuvant@AuNPs, Tc1, tumor microenvironments

Posted Date: July 29th, 2021

DOI: https://doi.org/10.21203/rs.3.rs-746366/v1

Abstract

Inducing tumor-specific T cell responses and regulating suppressive tumor microenvironments have been a challenge for effective tumor therapy. CpG (ODN), the Toll-like receptor 9 agonist, has been widely used as adjuvants of cancer vaccines to induce T cell responses. However, clinical benefits of CpG based tumor vaccine were limited primarily due to the poor targeting to lymph nodes. Here we developed a lipid-glycoadjuvant@AuNPs (LCpG) by covalent conjugation of CpG with lipid-glycopolymers, which could be rapidly transported to and retained longer in the lymphoid nodes than unmodified CpG. In melanoma model, LCpG controlled both primary tumor and its metastasis, and established long-term memory. In spleen and tumor draining lymphoid nodes, LCpG activated tumor-specific Tc1 responses, with increased $CD8^+$ T-cell proliferation, antigen–specific Tc1 cytokine production and specific-tumor killing capacity. In tumor microenvironments, antigen-specific Tc1 induced by the LCpG promoted CTL infiltration, skewed tumor associated macrophages to M1 phenotype, inhibited Treg differentiation and induced proinflammatory cytokines production in a CTL-derived IFN-γ-dependent manner. *In vivo* cell depletion and adoptive transfer experiments confirmed that antitumor activity of LCpG included vaccine was mainly dependent on CTL-derived IFN-γ. The anti-tumor efficacy of LCpG was dramatically enhanced when combined with anti-PD1 immunotherapy. Together, our results demonstrated that LCpG was a promising adjuvant for vaccine formulation which could augment tumor-specific Tc1 activity, and regulate tumor microenvironments.

1. Backgroud

Cancer immunotherapy, a concept by activating body's immune system to fight against cancers, is considered as one of the most promising therapeutic strategies for cancer [1]. It is universally accepted that a robust CTL response is required to clear the cancers. Various cancer immunotherapies have been designed to amplify CTL response such as cancer vaccines, immune checkpoint blockade, and adoptive T-cell transfer [2, 3]. However, these immunotherapies are effective in less than 30 percent of cancer patients [4]. One of the major factors involved in the low response rate are the lack of CTL infiltration in tumor bed (so-called "cold tumors") [5, 6]. Cancer vaccines are designed to activate and amplify tumor-specific T cells responses against tumor antigens, allowing CTL to migrate to TME and eradicate cancer cells [7]. However, immunosuppressive cells accumulated in TME rapidly suppress T cells by inhibiting T cell function and impairing their ability to produce proinflammatory cytokines such as TNFα and IFNγ [8–10]. Immunosuppressive populations accumulated in the TME include regulatory T cell (Treg), myeloid-derived suppressor cells (MDSCs), and tumor-associated macrophage (TAM). Thus, successful cancer immunotherapy relies on both priming functional tumor-specific T cells and regulating TME [12].

Dendritic cell (DC), the most effective antigen-presenting cell (APC), plays a central role in activation of T cells response [12]. For optimal T cell priming, DC requires signals from the interaction between its pattern recognition receptor (PRR) and pathogen-associated molecules, which activate DC and promote antigen presentation. Antigen presentation by immature DC often results in T cell anergy, which is a critical element of tumor escape [13]. Class B CpG-ODN, the TLR9 agonist, can engage TLR9 leading to

downstream signaling and activate DC, thus trigger T cell immune responses [14]. Although *in vitro* study exhibited the potential of CpG in promoting DC activation, but it has not been translated *in vivo*, primarily due to delivery efficacy, poor induction of DC maturation and safety concerns [15]. A numerous studies have proved that conjugation of CpG with other ligands of PRR expressed on DC may induce DC activation effectively [16]. Therefore, conjugating CpG with other PRR ligands and promoting its uptake by DC in peripheral lymphoid tissue are critical for its antitumor response in clinics, as these not only improve its immune-stimulating efficacy, but also greatly reduce its systemic toxicity.

To promote lymphoid-targeting capacity of CpG, we constructed lipid-glycoadjuvant@AuNPs (LCpG) by covalent conjugation of CpG with lipid-glycopolymers. In tumor-bearing mice, LCpG included vaccine strongly augmented antigen-specific Tc1 cells, promoted their infiltration in TME and regulated TME in a CTL-dependent induction of IFN-γ. Administration of the vaccine also significantly prevented lung metastasis of the tumor through similar mechanisms. The vaccine exhibited synergistic antitumor effects when combined with checkpoint blockade. Moreover, the combined therapies by vaccine and checkpoint blockade built memory response against secondary challenge of high dose tumor cells in a CTL-dependent manner. In conclusion, our study provides a novel adjuvant which may have general applicability to the development of vaccines against tumors.

2. Methods

2.2 Animals

Specific-pathogen-free (SPF) 6-week-old female C57BL/6 mice were obtained from the Shanghai Laboratory Animal Center (Shanghai, China), and kept under SPF conditions. All animal protocols were approved by the ethics committee of Soochow University according to the National Institutes of Health Guide for the Care and Use of Laboratory Animals. At the end of each *in vivo* experiment, mice were euthanized in a CO_2-containing chamber.

2.3 Cell lines

B16-OVA and B16-F10 cells were obtained from the American Type Culture Collection, and cultured in complete DMEM medium (Gibco) with 10% FBS. Cells were cytogenetically tested with negative.

2.4 Tumor models and vaccine treaments

There are four kinds of vaccines used in this study, including 10 ug OVA plus PBS (PBS + OVA), 10 ug OVA plus 1.24 nmol CpG (CpG + OVA), 10 ug OVA plus 1.24 nmol MCpG (MCpG + OVA), and 10 ug OVA plus 1.24 nmol LCpG (LCpG + OVA) in a total volume of 100 uL. In primary melanoma model, 2×10^5 B16-OVA cells were *s.c.* implanted into the right flank of each mouse. Vaccines were *s.c.* injected at the left flank 7 and 12 days post tumor inoculation, respectively. Tumor sizes were daily measured from day 9 post tumor inoculation, and calculated using the formula $V = (L\times W^2)/2$, where L is the length (longest dimension), and W is the width (shortest dimension).

In lung metastasis model, 8×10^5 B16-OVA were *i.v.* injected into each mouse from tail vein. Vaccines were *s.c.* injected at the left flank 7 and 12 days post tumor implantation. 7 days later, mice were sacrificed and the metastatic nodules in lung were counted.

2.5 Cell preparation from spleens and tumors

Splenocytes were prepared by filtering homogenized spleen through a 70-mm nylon mesh. TILs were isolated by processing the tumor tissues into single-cell suspensions, and lymphocytes were separated on a 40% Percoll (GE Healthcare) gradient. Red blood cells were lysed. $CD8^+$ T cells were isolated from spleen using EasySep™ Mouse $CD8^+$ T Cell Isolation Kit (Stemcell) according to the protocols.

2.6 Adoptive transfer experiment

8×10^5 B16-OVA were *i.v.* injected into each mouse from tail vein. On day 7, 3×10^6 $CD8^+$ T cells isolated from spleen of tumor-bearing mice treated with PBS or LCpG + OVA were *i.v.* injected into tumor-bearing mice. Mice were sacrificed and the metastatic nodules in lung were counted 12 days later.

2.7 T cell proliferation assay

Splenocytes were co-cultured with OVA protein for about 24 h, and irradiated with 200 Gy via a ^{60}Go source. 50,000 $CD4^+$ or $CD8^+$ T cells isolated from vaccine-treated mice were co-culture with above splenocytes for about 60 h. Then 10% CCK8 was added to each well and incubated for another 2 h. The absorbance was detected at OD450 nm. The stimulation index (SI) was calculated as: (OD450 of T cells stimulated with OVA-loading splenocytes - OD450 of Media)/ (OD450 of T cells stimulated with splenocytes - OD450 of Media).

2.8 Cytotoxicity assay

$CD8^+$ T and other populations of splenocytes (without $CD8^+$ T) were used as effector cells. Effector were diluted and cultured with B16-OVA (4,000 cells/well, target) in a 96-well plate at different effector/target ratios. Cytotoxicity was measured by CytoTox 96 nonradioactive cytotoxicity assay (Promega). The percentage of lysis was calculated using the following formula: (experimental - effector spontaneous - target spontaneous) × 100/(target maximum - target spontaneous).

2.9 Bone marrow DC (BMDC) generation

Briefly, bone marrow cells collected from the femur and tibia of mice were cultured in RPMI 1640 medium (containing 1% penicillin-streptomycin-glutamine, 50 μM 2-mercaptoethano, 10% FCS, 10 ng/mL GM-CSF, and 10 ng/mL IL-4). The medium was half-refreshed every 2 days. After 7 days of culture, the nonadherent and loosely adherent cells were harvested as BMDCs.

2.10 Flow cytometry

Monoclonal antibodies were purchased from BD Biosciences and Biolegend: anti-CD4-FITC (RM4-5), anti-NK1.1-FITC (PK136), anti-CD19-FITC (1D3), anti-CD3e-PE (145-2C11), anti-IL4-PE (11B11), anti-IFNγ-PE (XMG1.2), anti-CD8a-PerCP Cy5.5 (53 – 6.7), anti–Gr1-PE, anti–Gr1-PerCP Cy5.5 (RB6-8C5), anti-CD11b-

PE-Cy7 (M1/70), anti-CD44-PE (IM7), anti-CD45-APC (30-F11) anti-CD62L-FITC (MEL-14), anti-CD11c-PE-Cy7 (HL3), anti-Foxp3-APC, anti-F4/80-FITC (BM8), anti-CD16/32-PE (93), anti-CD206-PE (C068C2), anti-PD1-APC (29F.1A12), anti-MHC II-FITC and anti-TNFα-APC (MP6-XT22). Cells staining was performed in FACS buffer (PBS containing 1% BSA, 0.2 mM EDTA, and 0.1% NaN_3) supplemented with purified anti-CD16/32 for 30 min at 4°C. The flow cytometric results were analyzed with FACS CantoII (BD Biosciences) using CellQuest software.

2.11 Tetramer Staining

TILs were blocked with Fc-blocker and stained with PE-labeled tetramers (Beckman Coulter) and anti-CD8-APC for 30 min at room temperature. Cells were washed, resuspended in FACS buffer and analyzed with FACS CantoII (BD Biosciences).

2.12 m6A quantification

BMDCs were co-cultured with PBS + OVA, CpG + OVA, MCpG + OVA or LCpG + OVA for 24h. The total RNA were extracted and 200 ng total RNA of each sample was used for further analysis. The global m6A methylation of RNA level was measured by using the m6A RNA Methylation Assay Kit (Colorimetric) from Abcam (ab185912) according to the manufacturer's protocol.

2.13 Ex vivo co-culture assays

1.5×10^6 $CD8^+$ T cells were isolated from spleen and co-cultured with a single tumor cell suspension from untreated B16-OVA tumor-bearing mice. 10 ug/ml α-IFNγ (XMG1.2, Bioxcell) or α-TNFα (XT3.11, Bioxcell) were added in to the co-culture system as indicated.

2.14 In vivo cell depletion and cytokine neutralization

To deplete NK, $CD4^+$ or $CD8^+$ T cells, antibodies specific to NK1.1 (PK136, Bioxcell), CD4 (GK1.5, Bioxcell) or CD8 (53 – 6.7, Bioxcell) were used. To neutralize IFNγ or TNFα, α-IFNγ (XMG1.2, Bioxcell) or α-TNFα (XT3.11, Bioxcell) were used. For Each mouse was *i.p.* injected with 200ug of the specific antibodies 1 days before vaccine treatment, and the injections were repeated every 3 days. Macrophages depletion were performed by *i.p.* injection of 800 ug Clophosome (Anionic Liposomal Clodronate, FormuMax) 2 day before vaccination, and the injections were repeated 7 days later. The efficacy of cell depletion was confirmed by flow cytometric analysis.

2.15 Lymphatic transport and retention of modified-gold nanoparticle

Mice were injected subcutaneously in the dorsal toe of the hind paw with CpG plus gold nanoparticles or LCpG at a gold dose of 2 mg/kg body weight. Mice were euthanized at 2, 8 and 24 h post-administration, and the axillary lymph nodes were collected, cleaned and weighed. For ICP-MS analysis, the lymph nodes with the gold nanoparticles were dissolved by aqua regia (the volume ratio of 37% HCl and 70% HNO3 was 3:1). The total amount of gold in harvested lymph nodes after nanoparticle treatment was quantified by ICP-MS (ICP-MS 7500 CS, Agilent Technologies, USA).

2.16 In vitro activation of OVA-specific CD8 + T cells by vaccine-pulsed APCs

The mononuclear cells (1×10^6/ml) were cultured with either OVA, MCpG + OVA or LCpG + OVA (1 μg of OVA) for 2h at 37°C. The non-adherent cells were removed 24h later, and the remaining adherent cells were further cultured for 24 h at 37°C. Then 5×10^5 $CD8^+$ T cells isolated from the spleens of OT-I mice were added to these adherent cells. The supernatants were collected at 48 h, and the IFN-γ in the supernatant were quantified by ELISA according to the manufacturer's instructions.

2.17 Statistical analysis

Experiments were performed at a minimum of triplicate. Data were analyzed using a one-way analysis of variance (ANOVA) with the Tukey's post-hoc test for statistical evaluation. Data were analyzed using GraphPad Prism 8 software for Windows (GraphPad Software, San Diego, CA), and differences were considered statistically significant when $p < 0.05$. The significance levels are marked *$p < 0.05$, **$p < 0.01$, ***$p < 0.001$ and ****$p < 0.0001$.

3. Results

3.1 Immune stimulatory effects of Lipid-glycoadjuvant@AuNPs

To fabricate well-defined lipid-glycopolymer, the photo-induced reversible addition fragmentation chain transfer (RAFT) polymerization techniques and Cu(I)-catalyzed azidealkyne cycloaddition (CuAAC) reaction as well as NHS-ester chemistry were employed to design the desired polymers (Fig. 1A). The successful polymerization and click reaction with determined structures were confirmed by ^{1}H-NMR analysis. In addition, the actual molecular weight of polymers could be found in NMR (Figure S1-S4). Subsequently, lipid-glycoadjuvant@AuNPs were generated by using lipid-glycopolymer as reductant, $HAuCl_4$ as oxidant, and amine-terminal CpG (CpG-NH_2) as a bioactive agent. The UV-vis absorption spectrum, the transmission electron micrograph (TEM) image and dynamic light scattering (DLS) (Figures S5-S7) results indicated that novel lipid-glycoadjuvant@AuNPs were successfully fabricated. To investigate the lymphatic drainage of these adjuvants, mice were injected *s.c.* in the dorsal toe of the

fore/hind paw and the amounts of gold were detected by ICP-MS. At 2 h post-injection, both nanoparticles were rapidly transported to the lymph nodes. The amount of gold in the lymph nodes was significantly higher for subsequent time-points of animals injected with LCpG than non-conjugated controls. Gold concentrations in axillary lymph nodes from LCpG group increased even after 24 h, while gold concentrations of unconjugated gold decreased after 2 h (Fig. 1B). These results suggested that LCpG had improved uptake and retention in lymphoid nodes than unconjugated CpG.

DC is crucial for initiating adaptive immune responses. Co-cultured with LCpG significantly enhanced the expression of inflammatory cytokines (IL-12 and TNF-α) on DC (Fig. 1C&D). N6-methyladenosine (m^6A) modification plays important roles in various cellular responses by regulating mRNA biology. Co-culture with LCpG significantly increased mRNA m^6A methylation in DC (Fig. 1E). Previous study reported that m^6A modification was involved in DC maturation by affecting the translation of co-stimulatory molecules. LCpG included vaccine strongly enhanced the maturation of DC in TDLN by the up-expression of co-stimulatory molecules, MHCII and CD86 (Fig. 1F). When co-cultured with LCpG + OVA-treated BMDCs, IFN-γ produced by $CD8^+$ T cells from OT-1 mice was about 10-fold over PBS + OVA ($p < 0.0001$), 5-fold over CpG + OVA ($p < 0.001$) and 2-fold over MCpG + OVA ($p < 0.001$) (Fig. 1G). These results indicated that LCpG + OVA could activate antigen-specific CTL through promoting DC activation.

3.2 Inhibiting tumor growth by LCpG included vaccine is dependent on $CD8^+$ T-derived IFNγ

Malignant melanoma is hard to be cured by conventional therapy. To examine whether LCpG could be used as adjuvant for cancer immunotherapy, murine malignant melanoma models were generated by implantation of B16-F10. Tumor-bearing mice were treated with PBS plus B16 extract (PBS + B16), CpG plus B16 extract (CpG + B16), MCpG plus B16 extract (MCpG + B16) or LCpG plus B16 extract (LCpG + B16) at day 7 and 12 after tumor inoculation, respectively. LCpG significantly inhibited tumor growth when combined with tumor extract (Fig. 2A).

B16-OVA melanoma model is more suitable for analyzing adaptive response than B16-F10 melanoma model. Thus, we examined anti-tumor immunity of the vaccine on B16-OVA melanoma model in the subsequent study. On B16-OVA model, tumor-bearing mice were treated with PBS + OVA, CpG + OVA, MCpG + OVA or LCpG + OVA at day 7 and 12 after tumor inoculation, respectively. LCpG + OVA treatment greatly inhibited B16-OVA growth (Fig. 2B), as compared with PBS + OVA, CpG + OVA, MCpG + OVA (Fig. 2B). To determine whether the therapeutic effect of LCpG included vaccine is antigen specific, LCpG + OVA was also tested in mice bearing B16-F10 melanoma. LCpG + OVA didn't protect mice from B16-F10 challenging, indicating that the antitumor response induced by LCpG included vaccine was antigen specific (Fig. 2C).

NK and T cells are two major effectors against tumor by the innate and adaptive immunities, respectively. To determine which cells are critical for the antitumor effects induced by LCpG included vaccine, *in vivo* depletion of the specific cells was performed using specific Abs. Depletion of $CD8^+$ T cells completely

abrogated LCpG + OVA efficacy, whereas depletion of $CD4^+$ T or NK cells did not impair its efficacy, indicating that antitumor activity of LCpG included vaccine might be attributed to the $CD8^+$ T cells (Fig. 2D). The critical role of $CD8^+$ T cell in LCpG + OVA induced antitumor immunity was further confirmed by adoptive transferring experiments, where splenic $CD8^+$ T cell from LCpG + OVA treated mice effectively inhibit tumor growth (Fig. 2F). IFNγ and TNFα are two important cytokines for $CD8^+$ T cells function. To examine the role of the two cytokines in controlling tumor growth, neutralizing antibodies were used to block the two cytokines. Similar to $CD8^+$ T depletion treatment, anti-IFNγ treatment abrogated the therapeutic effects induced by LCpG + OVA, while anti-TNFα treatment had no obvious effect on LCpG + OVA efficacy, suggested that antitumor effects of $CD8^+$ T cells induced by LCpG + OVA might depend upon their secretion of IFNγ (Fig. 2E). An adoptive transfer experiment further confirmed that IFNγ secreted by $CD8^+$ T cells was required to their antitumor responses, where $CD8^+$ T cells from LCpG + OVA treated mice lost their therapeutic effects by anti-IFNγ treatments (Fig. 2F). Together, these results suggested that LCpG included vaccine inhibits tumor growth dependent on CTL and its secretion of IFNγ.

3.3 LCpG included vaccine promotes Tc1 response

To determine whether LCpG included vaccine could induce sufficient T cell responses, the function of T cells in tumor draining lymph nodes (TDLN) and spleen were measured 5 d after vaccine treatment. $CD8^+$ T cells in TDLN from LCpG + OVA treated tumor-bearing mice produced significantly high levels of IFNγ and TNFα relative to those from other vaccines treatment in response to OVA protein *ex vivo* (Fig. 3A). LCpG + OVA treatment also increased the $CD8^+$ T cells numbers and the prevalence of both IFNγ-produced $CD4^+$ and $CD8^+$ T cells in spleen (Fig. 3B). Tumor antigens can be transported to the TDLN to prime T cells. We found that the prevalence of $IFN\gamma^+CD8^+$ T cells in TDLN were significantly higher than those in spleen, indicating that $CD8^+$ T cells might be further primed in TDLN from tumor-bearing mice.

The proliferation of $CD8^+$ T cells in spleen was also enhanced after LCpG + OVA treatment (Fig. 3C). Direct killing is the main function of $CD8^+$ T cells in antitumor immunity. LCpG included vaccine strongly enhanced the tumor killing capacity of $CD8^+$ T cells, whereas CpG or PBS included vaccine could not enhance killing capacity of $CD8^+$ T cells ($p < 0.001$; Fig. 3D). Other populations from spleen (excluded $CD8^+$ T) had no obvious killing capacity (Fig. 3D). Together, these results illustrated that LCpG included vaccine augmented CTL activation and function in spleen and TDLN.

Trafficking into the tumor is required for T cells to eradicate tumors, and greater numbers of TILs, especially CTL, are associated with better survival outcomes in patients. $CD45^+$ TILs numbers per tumor weight in LCpG + OVA treated mice was significantly higher than those treated with PBS + OVA, CpG + OVA or MCpG + OVA ($p < 0.001$; Fig. 3E). The percentage of $CD4^+$ T in TIL was similar in each group (Fig. 3F). The percentage of $CD8^+$ T was also dramatically enhanced in TILs after LCpG + OVA treatment, as compared with PBS + OVA ($p < 0.001$), CpG + OVA ($p < 0.01$) or MCpG + OVA ($p < 0.05$) treatment (Fig. 3G). Tumor infiltrating $CD8^+$ T cells from LCpG + OVA-treated mice exhibited greatly enhanced IFNγ production

relative to those from PBS + OVA ($p < 0.0001$), CpG + OVA ($p < 0.0001$) or MCpG + OVA ($p < 0.01$) treatment (Fig. 3H). Additionally, prevalence of TNFα-produced $CD8^+$ T cells was increased after LCpG + OVA treatment relative to those with PBS + OVA ($p < 0.01$), CpG + OVA ($p < 0.05$) or MCpG + OVA ($p < 0.05$) treatment (Fig. 3H). Robust OVA^+ $CD8^+$ T cells response induced by LCpG + OVA was also confirmed by OVA tetramer analysis (Fig. 3I). These results demonstrated that LCpG + OVA treatment augmented tumor-specific Tc1 and promoted its infiltration in tumor sites.

3.4 Regulating TME by LCpG included vaccine in tumor-specific CTL-derived IFNγ-dependent manner

Solid tumors usually are infiltrated with abundant immunosuppressive cells, such as TAMs and Tregs. M1 macrophages are considered to be beneficial for antitumor immunity, whereas M2 cells lead to tumor progression. M1 macrophages expressed major histocompatibility complex class II (MHCII) and costimulatory molecules, such as CD80 and CD86, while M2 cells expressed a typical marker, CD206. LCpG + OVA treatment significantly increased $CD86^+MHCII^+$M1, and decreased $CD206^+$M2 (Fig. 4A&B). This phenotype was completely abrogated by $CD8^+$ T cell depletion or anti-IFNγ treatment (Fig. 4C&D). To determine whether $CD8^+$ T derived IFNγ could directly mediate M1 polarization, $CD8^+$ T cells were co-cultured with B16-OVA tumor suspension from untreated tumor-bearing mice *ex vivo*. $CD8^+$ T cells from LCpG + OVA treated mice increased M1 and decreased M2. Anti-IFNγ treatment abrogate the effects of $CD8^+$ T cells on M1 expansion, while CD206 expression was not significantly affected (Fig. 4E&F). The supernatants of tumor tissues from vaccine-treated mice were tested for IFNγ production by ELISA. LCpG + OVA treatment dramatically increased the production of IFNγ in TME, and depletion of $CD8^+$ T cells totally suppressed IFNγ production in TME, indicating that IFNγ production in TME was derived from $CD8^+$ T cells (Fig. 4M). Together, these data suggested that CTL was the main source of IFNγ in TME and that CTL derived IFNγ promote M1 TAMs.

Tumor-infiltrating Tregs suppressed local anti-tumor immune responses. LCpG + OVA treatment significantly decreased $CD4^+Foxp3^+$Treg frequency in TME (Fig. 4G). More and more study demonstrated that Treg infiltration alone was not associated with worse survival, whereas a high $CD8^+$/Treg ratio was found to be associated with improved survival. When combined with the increasing $CD8^+$ T prevalence, the ratio of $CD8^+$ T cells to Tregs was dramatically increased by 5-fold in response to LCpG + OVA treatment over the PBS + OVA ($p < 0.0001$), 3-fold over CpG + OVA ($p < 0.001$) and 1.8-fold over MCpG + OVA ($p < 0.01$) treatments (Fig. 4J). To examine whether $CD8^+$ T could regulate Tregs upon LCpG + OVA treatment, TILs from vaccine-treated mice were examined for Tregs prevalence by FACs. $CD8^+$ T cell depletion significantly increased Treg frequency (Fig. 4H) and decreased the ratio of $CD8^+$ T cells to Tregs in TILs from LCpG + OVA (Fig. 4J) treated mice, indicating that LCpG + OVA treatment suppressed Tregs in TME. To further determine whether IFNγ could regulate Tregs *in vivo*, Tregs prevalences and ratio of $CD8^+$ T cells to Tregs in TILs from αIFNγ treated tumor-bearing mice were analysed. Blocking IFNγ promoted Tregs population in LCpG + OVA treated mice (Fig. 4H). Surprisingly, αIFNγ treatment greatly reduced

prevalence of $CD8^+$ T cells in tumors from LCpG + OVA treated mice (Fig. 3I), indicating that CTL derived IFNγ was essential to the infiltration of CTL into tumor. These results suggested that CTL-derived IFNγ might regulate Tregs in TME.

To determine whether $CD8^+$ T derived IFNγ could directly inhibit Tregs differentiation, $CD8^+$ T cells were co-cultured with B16-OVA tumor suspension from untreated tumor-bearing mice *ex vivo*. $CD8^+$ T cells from LCpG + OVA treated mice decreased Tregs differentiation in the co-culture, but neutralization of IFNγ had no effect on its differentiation (Fig. 3K), suggesting that Tregs differentiation in TME is depended on $CD8^+$ T and indirectly on IFNγ. TNFα is another important cytokine of $CD8^+$ T. *Ex vivo* co-culture experiment demonstrated that TNFα could inhibit Tregs differentiation (Fig. 4L). Further, we detected TNFα level in TME. LCpG + OVA treatment significantly increased TNFα production TME, which could be totally suppressed by αCD8 or αIFNγ treatments (Fig. 4N). Therefore, IFNγ promoted TNFα production in TME by promoting $TNF\alpha^+CD8^+$ T infiltration, and thus suppressed Tregs differentiation.

3.5 LCpG included vaccine inhibits lung metastasis of melanoma

The development of metastasis is a major contributor to the mortality of cancer patients, and it is always hardly effectively controlled by conventional therapies. Therefore, we wondered if peptide vaccine using LCpG as adjuvant has therapeutic effects against metastatic cancer. B16-OVA cells were *i.v.* injected into mice from tail vein to build lung metastasis, and vaccines were given 7 and 12 days later. LCpG + OVA treatment dramatically reduced the number of lung metastases relative to PBS + OVA ($p < 0.001$), CpG + OVA ($p < 0.01$) or MCpG + OVA ($p < 0.05$) treatment (Fig. 5A). The reduction of lung metastases was also correlated with an increase in survival (Fig. 5B). T cell responses induced by LCpG + OVA were also tested in metastasis model by flow cytometry on day 17 after tumor injection. Consistent with primary model, the percentages of tumor infiltrating $CD8^+$ T cells (Fig. 5C) and their production of both $IFN\gamma^+$ (Fig. 5D) and $TNF\alpha^+$T (Fig. 5E) were significantly increased after LCpG + OVA treatment. The significantly high infiltration of antigen-specific $CD8^+$ T cell upon LCpG + OVA treatment was also confirmed by OVA tetramer analysis (Fig. 5F).

The TME phenotype was also examined in metastasis model. Consistent with results in primary tumor model, the therapeutic effects induced by LCpG + OVA depended upon Tc1 and its secretion of IFNγ (Fig. 5G). LCpG + OVA treatment also skewed TAMs to M1 (Fig. 5H&I), inhibited Tregs and promote $CD8^+$ T/Tregs ratio in TME, and thus regulated TME in metastasis model. Together, these data demonstrated that LCpG included vaccine inhibited metastasis by promoting IFNγ production in Tc1 and regulating TME.

3.6 Synergistic effects and memory response induced by LCpG included vaccine combined with anti-PD-1 treatments depends upon CTL

Programmed death 1 (PD-1), one of immune checkpoint, is a critical negative regulator of T cell function, and blockade of PD-1 by antibody has been widely used in the clinic. To enhance the therapeutic efficacy of tumor vaccines, the combination treatment by both LCpG + OVA and blockade of PD-1 using αPD-1 was tested in primary tumor model. Blocking PD-1 could not provide therapeutic benefits, as compared with PBS + OVA treatment. In contrast, LCpG + OVA combined with PD-1 blocking resulted in synergistic effects in control tumor growth. Importantly, 9 out of 15 mice were completely protected from tumor growth by the combining treatments, whereas all the mice developed metastasis without combining therapies ($p < 0.001$; Fig. 6A). The therapeutic effects induced by LCpG + OVA combined with αPD-1 were totally abrogated with αCD8 treatment, illustrating the essential role of CTL in protecting mice from tumor by the combining therapies of vaccine and checkpoint blockade.

To test whether the survivors (mice cured by LCpG + OVA combined with PD-1 blockade treatment) from primary melanoma could develop memory response, survivor and naïve mice were *i.v.* injected with 1.6×10^6 B16-OVA at day 50 post *s.c.* implantation of melanoma. None of the survivors developed lung metastasis at day 14, while all of the naïve mice developed lung metastasis ($p < 0.001$; Fig. 6B). These results suggested that survivor from vaccine treatments developed memory response. To examine the role of $CD8^+$ T cell in the memory response, $CD8^+$ T cell were depleted in the rechallenging model. Depletion of $CD8^+$ T cells in the survivors greatly increased the lung metastasis ($p < 0.001$; Fig. 6B), illustrated the essential role of CTL in controlling tumor growth during the memory response. Notably, depleting of both macrophages by Clophosome and $CD8^+$ T cell totally abrogated the whole therapeutic effects from pre-existing CTL effects, suggested that the regulating of TME is also important for antitumor therapy induced by LCpG included vaccine. Thus, our data demonstrated that LCpG included vaccine promoted tumor-specific CTL responses, which regulated TME and elicited both primary and memory responses against cognate tumors.

4. Discussion

In present study, a novel adjuvant LCpG was developed by covalent conjugation of CpG to gold nanoparticles conjugated with mannose and lipids. The designed adjuvant could be rapidly transported to and retained longer in the lymphoid nodes, and promoted DC maturation. In melanoma model, LCpG controlled both primary melanoma and its metastasis, and established long-term memory dependent upon tumor specific Tc1 response. In tumor microenvironments, antigen-specific Tc1 induced by the LCpG skewed tumor associated macrophages to M1 phenotype, inhibited Treg differentiation and induced proinflammatory cytokines production in a CTL-derived IFN-γ-dependent manner (Fig. 7).

T cell immunity is the key mechanism of antitumor effect. CTLs recognize MHC I and peptide complex expressed on tumor cells, and lyse them directly. Thus, immunotherapy aims to promote CTL response. However, most of the immunotherapies result in low response rate, due to the formation of “cold tumors”. The main mechanisms involved in the formation of “cold tumors” include poor for providing costimulatory signals for T cell priming by APCs and deficit of T cell homing into the tumor bed [17]. DC, the most effective APC, plays a central role in activating T cells by providing TCR ligand, costimulatory

molecules and cytokines. During T cell priming, DC need to be activated and become matured first. m^6A is the most prevalent modification of eukaryotic RNA involved in various cellular responses by regulating mRNA biology [18]. RNA m^6A modification is essential for DC activation by promoting the expression of co-stimulatory molecules CD40, CD80 and cytokine IL-12 [19]. LCpG dramatically promoted RNA m^6A of DC, in comparison to uncongugated CpG. The advantages of LCpG on activating DC can be translated *in vivo*. In tumor-bearing mice, LCpG promotes DC activation by upregulated MHC II and B7 molecules expression on its surface. B7, the ligand of CD28, is the most important costimulatory molecules for T cell priming [20]. All these results demonstrate that LCpG is a promising adjuvant to activate T cell response by promoting DC activation.

$CD8^+$ T cells can be activated in two different ways to become cytotoxic effector cells. The one is mediated by the help from Th cells, and another is mediated directly by DC which has high intrinsic co-stimulatory activity [21, 22]. The simpler manner of CTL activation is priming by activated dendritic cells directly. Therefore, any adjuvants which can greatly upregulate co-stimulatory on DC, have the potential to primed CTL directly. Although Th cells were activated by LCpG, depletion of $CD4^+$ T cells didn't reduce the therapeutic effects provided by CTL, suggested that LCpG could stimulate CTL response directly by matured DC. Following the T cell priming, cytokines drive the differentiation of effector T subtypes. IL-12 has been found to be essential for Tc1 differentiation [23], and LCpG treatment greatly increased the expression of IL-12, which was consistent with the augment of Tc1 *in vivo*. Thus, LCpG can activate Tc1 irrespective of Th activation, demonstrating its broad potential for cancer immunotherapy.

Although tumor-infiltrating CTLs can recognize and destroy tumor cells directly, most of CTLs infiltrating in tumor are dysfunctional and impaired in their ability to secret proinflammantory cytokines such as IFNγ and TNFα [24, 25]. In present work, LCpG included vaccine greatly increased CTLs infiltration in tumor, and enhanced their ability to produce both IFNγ and TNFα in TME. IFNγ is a key effector molecule with pleiotropic effects in TME during anti-tumor immunity [26, 27]. It stimulates tumor cells to upregulate peptide-MHC I complex, the ligand for TCR, and thus enhances the immunogenicity of cancer [28]. It also triggers the production of chemokines, such as CXCL9, CXCL10 and CXCL11, to promote the recruitment of effector immune cells to the tumor sites [29, 30]. Our data reveled that neutralization of IFNγ dramatically decreased CTL trafficking to tumor, and reduced the totally therapeutic benefits from LCpG treatment. The antitumor effects of CTL adoptive transferring also abrogated after anti-IFNγ treatment, suggesting the essential role of IFNγ during CTL recruitment and anti-tumor immunity. IFNγ is also known to be one of the key inducers of M1 polarization [31]. M1 macrophages expressed high level of B7 molecules, such as CD80 and CD86 [32], and many recent works have emphasized the positive impact of M1 TAMs on survival of cancer patients [33, 34]. Consistently, LCpG treatment promoted M1 polarization in tumor sites dependent upon CTL-derived IFNγ. Although, LCpG treatment increased Th1 in tumor bed, the most amounts of IFNγ in TME were produced by CTL instead of Th1, as the lack of peptide-MHCII complex, the ligand of Th cell, in tumor beds.

Tregs can contribute to tumor immune evasion by suppressing CTL function [35]. Foxp3, a forkhead/winged helix transcription factor, which is crucial for the development of Tregs, is the most reliable marker for Tregs [36]. It is reported that TNFα has divergent effects on regulatory T cells [37]. LCpG treatment promoted TNFα production in TME, and the most amounts of TNFα were secreted by infiltrating CTL. The increasing of TNFα in TME was correlated with the decreasing of infiltrating Treg populations. *Ex vivo* study confirmed the essential role of TNFα in inhibiting Treg differentiation, which is consistent with the former study that TNFα could inhibit FoxP3 transcription [38, 39]. Neutralization of TNFα didn't reduce the therapeutic benefits from LCpG treatment, suggested that inhibiting Treg was not essential for the vaccine treatment.

It has been reported that tumor infiltrating CTLs have been associated with favorable clinical outcomes in a variety of cancers. However, these infiltrating CTLs may be actively restrained by inhibitory molecules expressed on their surface, such as PD-1 [40]. Blocking PD-1 signaling pathway has been tested in multiple cancer [41]. However, despite the success of monotherapies of blocking PD-1 in some cancers, most patients do not have durable clinical benefit. A major reason for the poor responding to PD-1 blocking therapy is the lack of CTL infiltration in the tumors. Our data demonstrated that melanoma-bearing mice treated with PBS + OVA had very low infiltration of $CD8^+$T cells in TME. The relative low CTL infiltration may be caused by the lack of adjuvant to activate DC, revealed by low expression level of costimulatory B7 molecules and IL-12 after PBS + OVA treatment. This kind of "cold tumor" did not respond to PD-1 blockade treatment effectively. On the contrary, LCpG included vaccine greatly enhanced $CD8^+$T cells accumulation in TME, which provided the targets for PD-1 blockade therapy, and thus combining LCpG included vaccine and anti-PD-1 therapy resulted in a synergistic effect in controlling tumor growth. Reduction of the benefits by $CD8^+$ T cells depletion confirms that CTL is the target for PD-1 blockade strategies. Taken together, we demonstrated that LCpG inclusion in vaccine formulations activated Tc1 responses *in vivo* and regulating TME in a TCL-derived IFNγ-dependent manner. Further studies are required to fully understand superior activity of LCpG in preclinical models.

Conclusion

Covalent conjugation with lipid-glycopolymers enhanced the lymphoid node-targeting of CpG and promoted its effect on DC maturation. The conjugated CpG activates tumor-specific Tc1 responses and regulates TME by skewing tumor associated macrophages to M1 phenotype, inhibiting Treg differentiation and inducing proinflammatory cytokines production in a CTL-derived IFN-γ-dependent manner. Together, the designed CpG is a powerful adjuvant for cancer immunotherapy.

Abbreviations

APC: antigen-presenting cell

DC: dendritic cell

PRR: pattern recognition receptor

ODN: synthetic oligodeoxynucleotide

Th: T helper cell

Tc: cytotoxic T cell

NK: nature killer

MDSC: meyloid-derived suppressor cell

OVA: ovalbumin

MHC: major histocompatibility complex

TLR: toll like receptor

TME: tumor microenvironments

TAM: tumor associated macrophage

Treg: regulatory T cells

PD-1: program death-1

IFN: Interferon

TNFα: tumor necrosis factor

Declarations

Ethics approval: All animal protocols were approved by the ethics committee of Soochow University according to the National Institutes of Health Guide for the Care and Use of Laboratory Animals.

Consent for publication: Not applicable.

Availability of data and materials: All data generated or analyzed during this study are included in this published article [and its supplementary information files]

Competing interests: The authors declare that they have no competing interests

Funding: This work has been supported by grants from the National Natural Science Foundation of China (grant numbers 31870918, 31500746), Open Project Program of Jiangsu Key Laboratory of Zoonosis (grant numbers R1906), Project Funded by the Priority Academic Program Development of Jiangsu

Higher Education Institutions, and the fifth batch of Suzhou health personnel training project (grant numbers GSWS2019073).

Authors' contributions: Xiaojing Xu, Cheng Yi and Youzhen Ge performed and interpreted the animal experiments. Tianyun Feng and Cenhao Wu analyzed T cell function. Mengjie Liu characterized the nanoparticles. Xiang Chen helped write the manuscript. Lixiang Zhao, Jun Zou and Weidong Zhang designed the research. All authors read and approved the final manuscript.

Acknowledgements: Not applicable.

References

1. Hegde PS, Chen DS. Top 10 Challenges in Cancer Immunotherapy. Immunity. 2020;52:17-35.
2. Tan S, Li D, Zhu X. Cancer immunotherapy: Pros, cons and beyond. Biomed Pharmacother. 2020;124:109821.
3. Waldman AD, Fritz JM, Lenardo MJ. A guide to cancer immunotherapy: from T cell basic science to clinical practice. Nat Rev Immunol. 2020;20:651-668.
4. Li HY, McSharry M, Bullock B, Nguyen TT, Kwak J, Poczobutt JM, *et al*. The Tumor Microenvironment Regulates Sensitivity of Murine Lung Tumors to PD-1/PD-L1 Antibody Blockade. Cancer Immunol Res. 2017;5:767-777.
5. Bonaventura P, Shekarian T, Alcazer V, Valladeau-Guilemond J, Valsesia-Wittmann S, Amigorena S, *et al*. Cold Tumors: A Therapeutic Challenge for Immunotherapy. Front Immunol. 2019;10:168.
6. Galon J, Bruni D. Approaches to treat immune hot, altered and cold tumours with combination immunotherapies. Nat Rev Drug Discov. 2019;18:197-218.
7. Thomas S, Prendergast GC. Cancer Vaccines: A Brief Overview. Methods Mol Biol. 2016;1403:755-61.
8. Zarour HM. Reversing T-cell Dysfunction and Exhaustion in Cancer. Clin Cancer Res. 2016;22:1856-64.
9. Saleh R, Toor SM, Sasidharan Nair V, Elkord E. Role of Epigenetic Modifications in Inhibitory Immune Checkpoints in Cancer Development and Progression. Front Immunol. 2020;11:1469.
10. Olivo Pimentel V, Yaromina A, Marcus D, Dubois LJ, Lambin P. A novel co-culture assay to assess anti-tumor CD8(+) T cell cytotoxicity via luminescence and multicolor flow cytometry. J Immunol Methods. 2020;487:112899.
11. Rahma OE, Hodi FS. The Intersection between Tumor Angiogenesis and Immune Suppression. Clin Cancer Res. 2019;25:5449-5457.
12. Gardner A, Ruffell B. Dendritic Cells and Cancer Immunity. Trends Immunol. 2016;37:855-865.
13. Macián F, Im SH, García-Cózar FJ, Rao A. T-cell anergy. Curr Opin Immunol. 2004;16:209-16.
14. Reilley MJ, Morrow B, Ager CR, Liu A, Hong DS, Curran MA. TLR9 activation cooperates with T cell checkpoint blockade to regress poorly immunogenic melanoma. J Immunother Cancer. 2019;7:323.

15. Scheiermann J, Klinman DM. Clinical evaluation of CpG oligonucleotides as adjuvants for vaccines targeting infectious diseases and cancer. Vaccine. 2014;32:6377-89.
16. Jung, H., Yu, G., Mok, H. CpG oligonucleotide and α-D-mannose conjugate for efficient delivery into macrophages. Appl Biol Chem. 2016;59:759-763.
17. Liu YT, Sun ZJ. Turning cold tumors into hot tumors by improving T-cell infiltration. Theranostics. 2021;11:5365-5386.
18. Zhang C, Fu J, Zhou Y. A Review in Research Progress Concerning m6A Methylation and Immunoregulation. Front Immunol. 2019;10:922.
19. Wang H, Hu X, Huang M, Liu J, Gu Y, Ma L, *et al*. Mettl3-mediated mRNA m(6)A methylation promotes dendritic cell activation. Nat Commun. 2019;10(1):1898.
20. Esensten JH, Helou YA, Chopra G, Weiss A, Bluestone JA. CD28 Costimulation: From Mechanism to Therapy. Immunity. 2016;44(5):973-88.
21. Wiesel M, Joller N, Ehlert AK, Crouse J, Spörri R, Bachmann MF, *et al*. Th cells act via two synergistic pathways to promote antiviral CD8+ T cell responses. J Immunol. 2002;168:3493-501.
22. Miah MA, Yoon CH, Kim J, Jang J, Seong YR, Bae YS. CISH is induced during DC development and regulates DC-mediated CTL activation. Eur J Immunol. 2012;42:58-68.
23. Camporeale A, Boni A, Iezzi G, Degl'Innocenti E, Grioni M, Mondino A, *et al*. Critical impact of the kinetics of dendritic cells activation on the in vivo induction of tumor-specific T lymphocytes. Cancer Res. 2003;63:3688-94.
24. Farhood B, Najafi M, Mortezaee K. $CD8^+$ cytotoxic T lymphocytes in cancer immunotherapy: A review. J Cell Physiol. 2019;234:8509-8521.
25. Bauer CA, Kim EY, Marangoni F, Carrizosa E, Claudio NM, Mempel TR. Dynamic Treg interactions with intratumoral APCs promote local CTL dysfunction. J Clin Invest. 2014;124:2425-40.
26. Dillinger B, Ahmadi-Erber S, Lau M, Hoelzl MA, Erhart F, Juergens B, *et al*. IFN-gamma and tumor gangliosides: Implications for the tumor microenvironment. Cell Immunol. 2018;325:33-40.
27. Thibaut R, Bost P, Milo I, Cazaux M, Lemaître F, Garcia Z, *et al*. Bystander IFN-gamma activity promotes widespread and sustained cytokine signaling altering the tumor microenvironment. Nat Cancer. 2020;1:302-314.
28. Zhou F. Molecular mechanisms of IFN-gamma to up-regulate MHC class I antigen processing and presentation. Int Rev Immunol. 2009;28:239-60.
29. Kanda N, Shimizu T, Tada Y, Watanabe S. IL-18 enhances IFN-gamma-induced production of CXCL9, CXCL10, and CXCL11 in human keratinocytes. Eur J Immunol. 2007;37:338-50.
30. Laing KJ, Bols N, Secombes CJ. A CXC chemokine sequence isolated from the rainbow trout Oncorhynchus mykiss resembles the closely related interferon-gamma-inducible chemokines CXCL9, CXCL10 and CXCL11. Eur Cytokine Netw. 2002;13:462-73.
31. Huang Y, Tian C, Li Q, Xu Q. TET1 Knockdown Inhibits Porphyromonas gingivalis LPS/IFN-gamma-Induced M1 Macrophage Polarization through the NF-kappaB Pathway in THP-1 Cells. Int J Mol Sci.

2019;20:2023.
32. Mahon OR, Kelly DJ, McCarthy GM, Dunne A. Osteoarthritis-associated basic calcium phosphate crystals alter immune cell metabolism and promote M1 macrophage polarization. Osteoarthritis Cartilage. 2020;28(5):603-612.
33. Macciò A, Gramignano G, Cherchi MC, Tanca L, Melis L, Madeddu C. Role of M1-polarized tumor-associated macrophages in the prognosis of advanced ovarian cancer patients. Sci Rep. 2020;10(1):6096.
34. Ino Y, Yamazaki-Itoh R, Shimada K, Iwasaki M, Kosuge T, Kanai Y, *et al*. Immune cell infiltration as an indicator of the immune microenvironment of pancreatic cancer. Br J Cancer. 2013;108(4):914-23.
35. Najafi M, Farhood B, Mortezaee K. Contribution of regulatory T cells to cancer: A review. J Cell Physiol. 2019;234:7983-7993.
36. Sayed D, El-Badawy OH, Eldin EN, Bakry R, Badary MS, Abd-Alrahman ME, *et al*. Is Foxp3 a good marker for regulatory T cells? Egypt J Immunol. 2014;21(2):1-8.
37. Mehta AK, Gracias DT, Croft M. TNF activity and T cells. Cytokine. 2018;101:14-18.
38. Nie H, Zheng Y, Li R, Guo TB, He D, Fang L, *et al*. Phosphorylation of FOXP3 controls regulatory T cell function and is inhibited by TNF-alpha in rheumatoid arthritis. Nat Med. 2013;19(3):322-8.
39. Valencia X, Stephens G, Goldbach-Mansky R, Wilson M, Shevach EM, Lipsky PE. TNF downmodulates the function of human CD4+CD25hi T-regulatory cells. Blood. 2006;108:253–61.
40. Duraiswamy J, Kaluza KM, Freeman GJ, Coukos G. Dual blockade of PD-1 and CTLA-4 combined with tumor vaccine effectively restores T-cell rejection function in tumors. Cancer Res. 2013;73:3591-603.
41. Philips GK, Atkins M. Therapeutic uses of anti-PD-1 and anti-PD-L1 antibodies. Int Immunol. 2015;27:39-46.

Figures

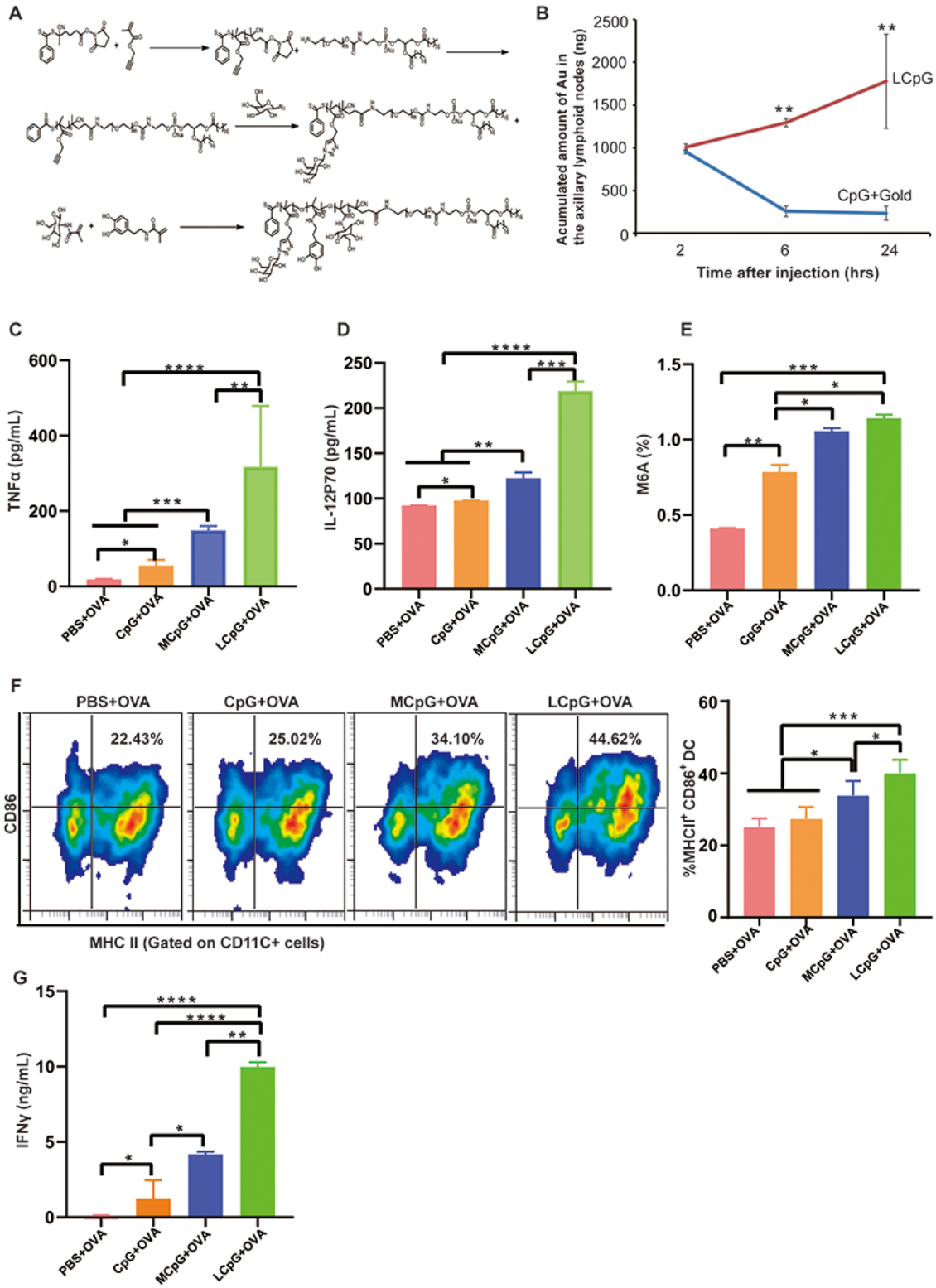

Figure 1

Immune stimulatory effects of Lipid-glycoadjuvant@AuNPs. (A) Fabrication of lipid-glycopolymers by the combination of photo-induced RAFT polymerization and click chemistry. (B) ICP-MS quantitative data of gold in axillary lymph nodes, comparing unconjugated gold nanoparticles plus CpG and LCpG at different time points post-injection. Co-cultured DC with PBS+OVA, CpG+OVA, MCpG+OVA or LCpG+OVA for 12h, and the amounts of TNF-α (C) and IL-12P70 (D) in the supernatants were detected by ELISA. (E) BMDCs

were co-cultured with PBS+OVA, CpG+OVA, MCpG+OVA or LCpG+OVA for 24h. The total RNA were extracted and 200 ng total RNA of each sample was used for m6A qualification. (F) Melanoma-bearing mice were immunized with BS+OVA, CpG+OVA, MCpG+OVA or LCpG+OVA, and the expression of MHCII and CD86 on DC were detected by FACS 3 days later. (G) Vaccine-pulsed APCs were cultured with CD8+ T cells isolated from OT-I mouse spleens for 48 h, and the IFNγ levels in the supernatants were analyzed by ELISA. *p < 0.05 and **p < 0.01, ***p < 0.001 and ****p < 0.0001.

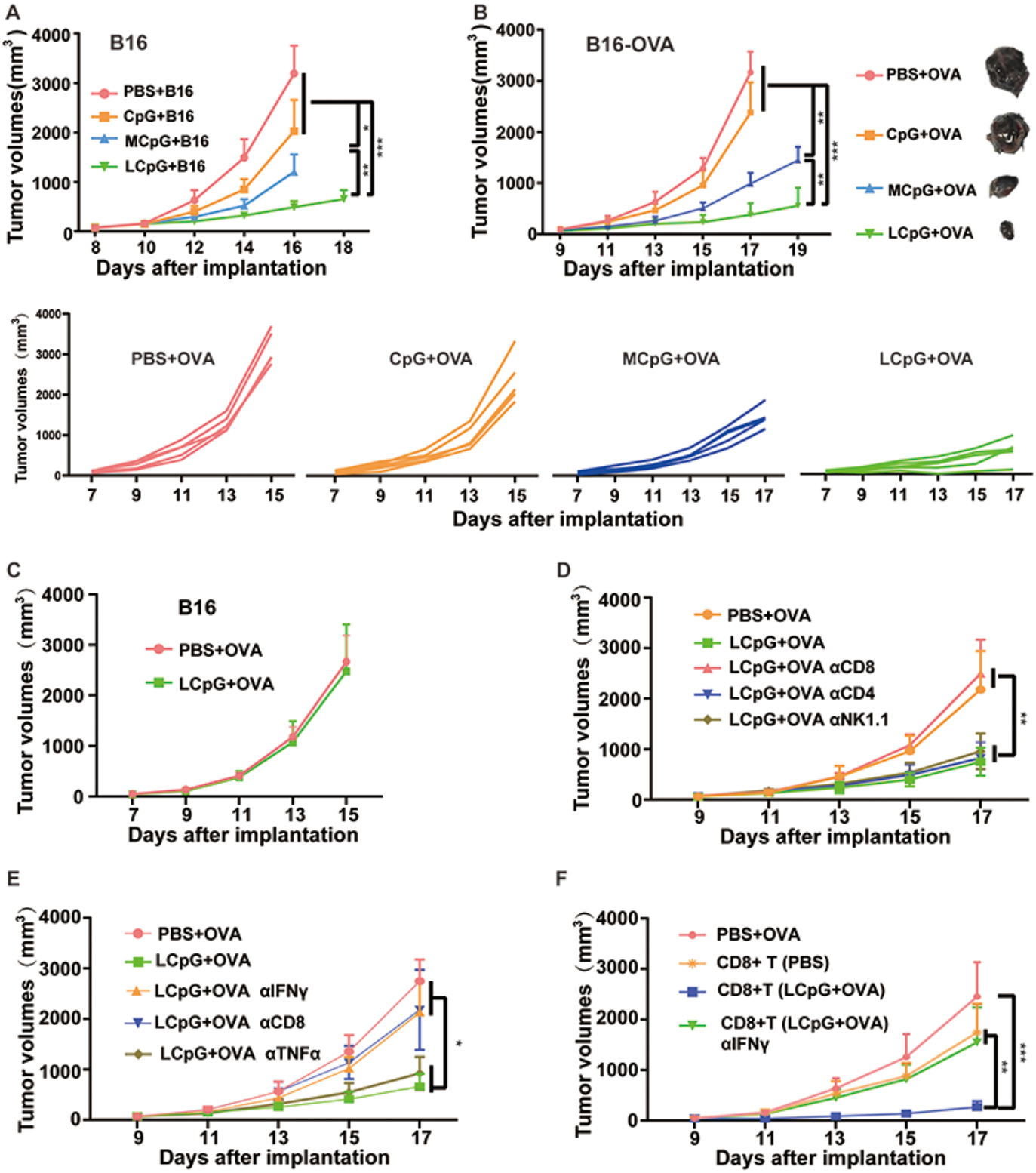

Figure 2

LCpG included vaccine inhibits melanoma in a CD8+ T cell-derived IFNγ dependent manner. (A) Tumor growth curves of mice implanted with B16 cells. Mice were injected s.c. with 1×105 B16. At day 7 and 12 post tumor inoculation, mice were immunized with B16 extract plus different adjuvants (CpG, MCpG, LCpG) or PBS. The tumor volumes were monitored. (B) Tumor growth curves of mice implanted with B16-OVA cells. Mice were injected s.c. with 1.5×105 B16-OVA. At day 7 and 12 post tumor inoculation, mice were immunized with OVA protein plus different adjuvants (CpG, MCpG, LCpG) or PBS. The tumor volumes were monitored. (C) Mice implanted with B16 cells were received PBS+OVA or LCpG+OVA treatment. The tumor volumes were monitored. (D) Tumor curve of vaccine-treated mice were injected i.p. with 1 mg GK1.5 (anti-mouse CD4 mAb), 53-6.7 (anti-mouse CD8 mAb) or PK136 (anti-mouse NK1.1 mAb) 2 days before the first immunization, and the injections were repeated 7 days later. The tumor volumes were monitored. (E) Tumor curve of vaccine-treated mice were injected i.p. with 1 mg 53-6.7 (anti-mouse CD8 mAb), XMG1.2 (anti-mouse IFNγ mAb) or XT3.11 (anti-mouse TNFα mAb) 2 days before the first immunization, and the injections were repeated 7 days later. The tumor volumes were monitored. (F) Mice bearing B16-OVA tumor were adoptively transferred with 3 × 106 CD8+ T cells from PBS+OVA or LCpG+OVA treated mice. *$p < 0.05$ and **$p < 0.01$, ***$p < 0.001$ and ****$p < 0.0001$.

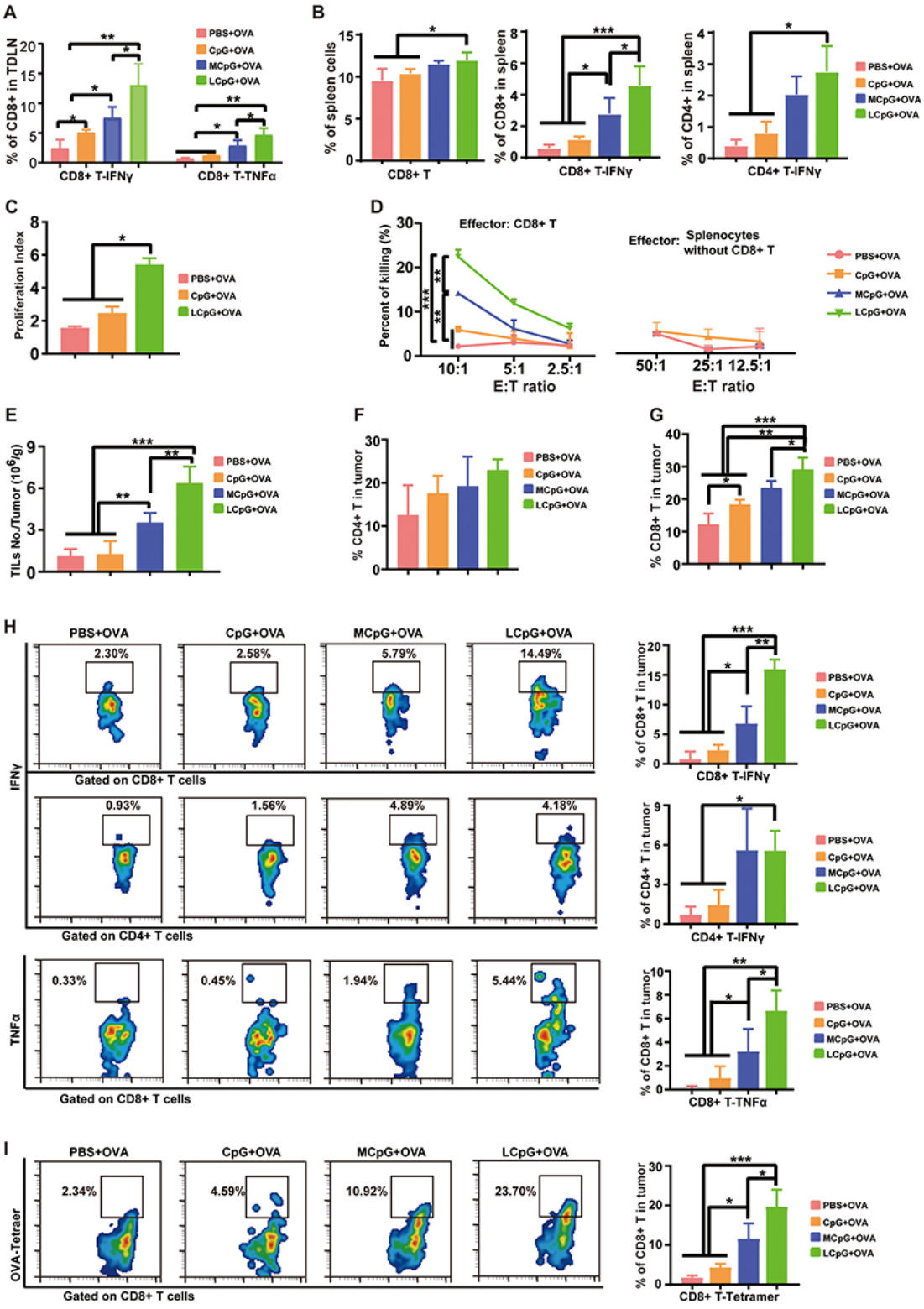

Figure 3

LCpG included vaccine promotes TC1 responses. Mice were injected s.c. with 1.5×105 B16-OVA. At day 7 and 12 post tumor inoculation, mice were immunized with different vaccines. Seven days later, mice were sacrificed, and the spleens, TDLNs and tumors were collected. (A) Frequency of IFNγ+ or TNFα+ CD8+T in TDLN. (B) Cell numbers, frequencies of CD8+ T cells and IFNγ+ CD4+ or CD8+ T cells in spleen. (C) Proliferations of CD8+ T cells isolated from spleen were determined using CCK8 cell counting kits. The

stimulation index (SI) is calculated as the ratio of the proliferation of cells received OVA-specific stimulation to cells without OVA-specific stimulation in the same group. (D) Cytotoxicity assay of splenic CD8+ T cells and other population without CD8+ T cells from the tumor-bearing mice against B16-OVA tumor cells. The specific killings were determined using CytoTox 96 nonradioactive cytotoxicity assay. (E-G) Total numbers of TILs and percentages of CD4+ and CD8+ T cells in TILs. (H) Intracellular staining of IFNγ and TNFα production on CD8+ and CD4+ T cells from TILs stimulated with OVA. (I) Tetramer staining of OVA–specific CD8+ T cells in TILs. *p < 0.05 and **p < 0.01, ***p < 0.001 and ****p < 0.0001.

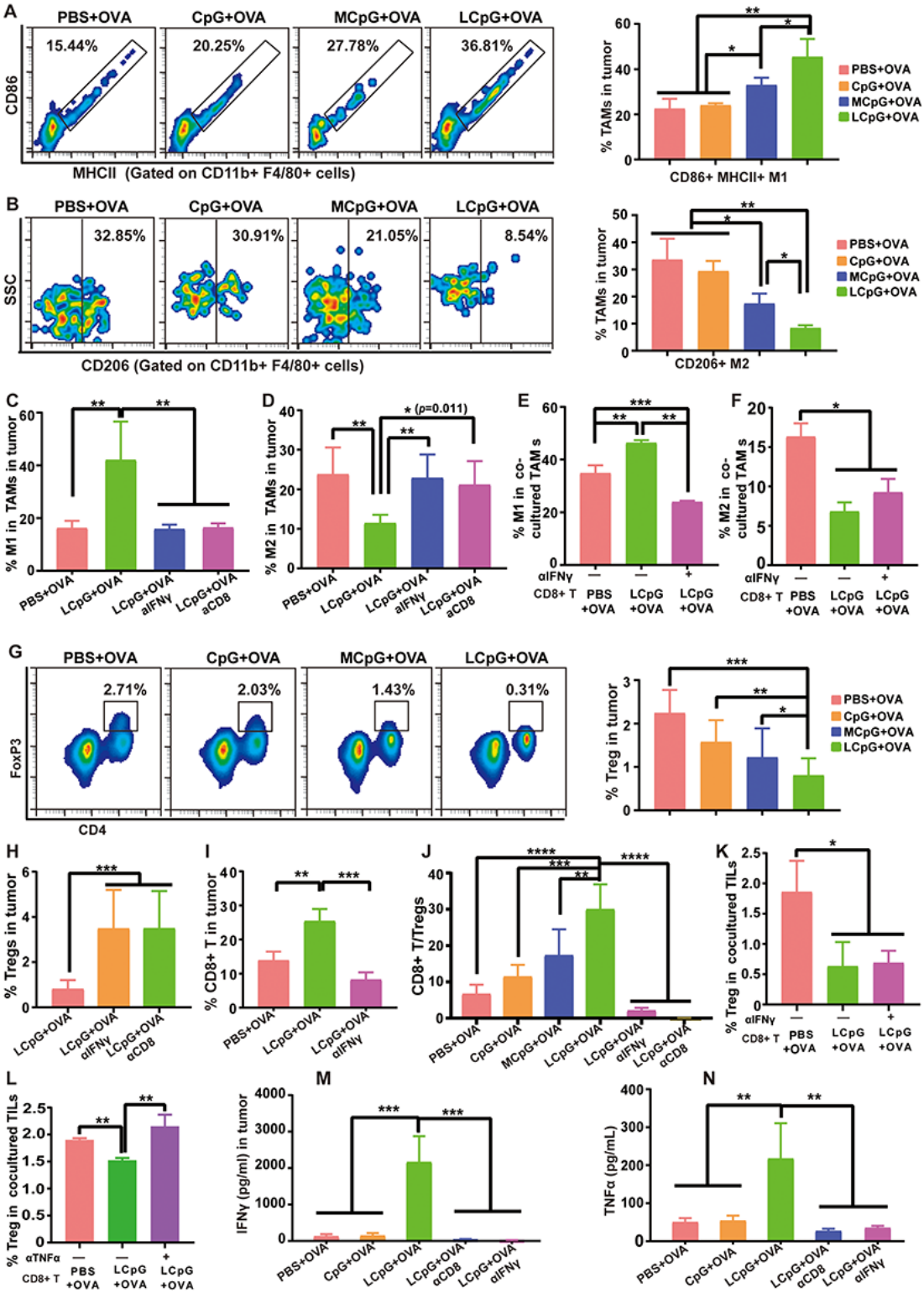

Figure 4

Regulating tumor microenvironment by LCpG is dependent on ctl-derived IFNγ. Mice were injected s.c. with 1.5×105 B16-OVA. At day 7 and 12 post tumor inoculation, mice were immunized with different vaccines. Mice were treated with anti-CD8, anti-IFNγ or anti-TNFα, on day 6 and repeated every 3 days when indicated. Seven days after the last immunization, mice were sacrificed, and the TILs were isolated and analyzed by FACs. On day 11 in the TME. (A-D) Frequency of M1 (CD86+ MHCII+) and M2 (CD206+) macrophages were detected by FACS. (E&F) Purified splenic CD8+ T cells from LCpG+OVA–treated or PBS+OVA-treated B16-OVA tumor-bearing mice were co-cultured with an untreated B16-OVA tumor suspension with or without 10 μg/mL IFNγ for 24 h. (G&H) Frequency of Treg in TILs were detected by FACS. (I) Frequency of CD8+ T in TILs. (J) CD8/Treg ratio. (K&L) Purified splenic CD8+ T cells from LCpG+OVA–treated or PBS+OVA-treated B16-OVA tumor-bearing mice were co-cultured with an untreated B16-OVA tumor suspension with or without 10 μg/mL IFNγ or TNFα for 24 h. (M&N) IFNγ and TNFα levels in supernatants of tumor detected by ELISA. *$p < 0.05$ and **$p < 0.01$, ***$p < 0.001$ and ****$p < 0.0001$.

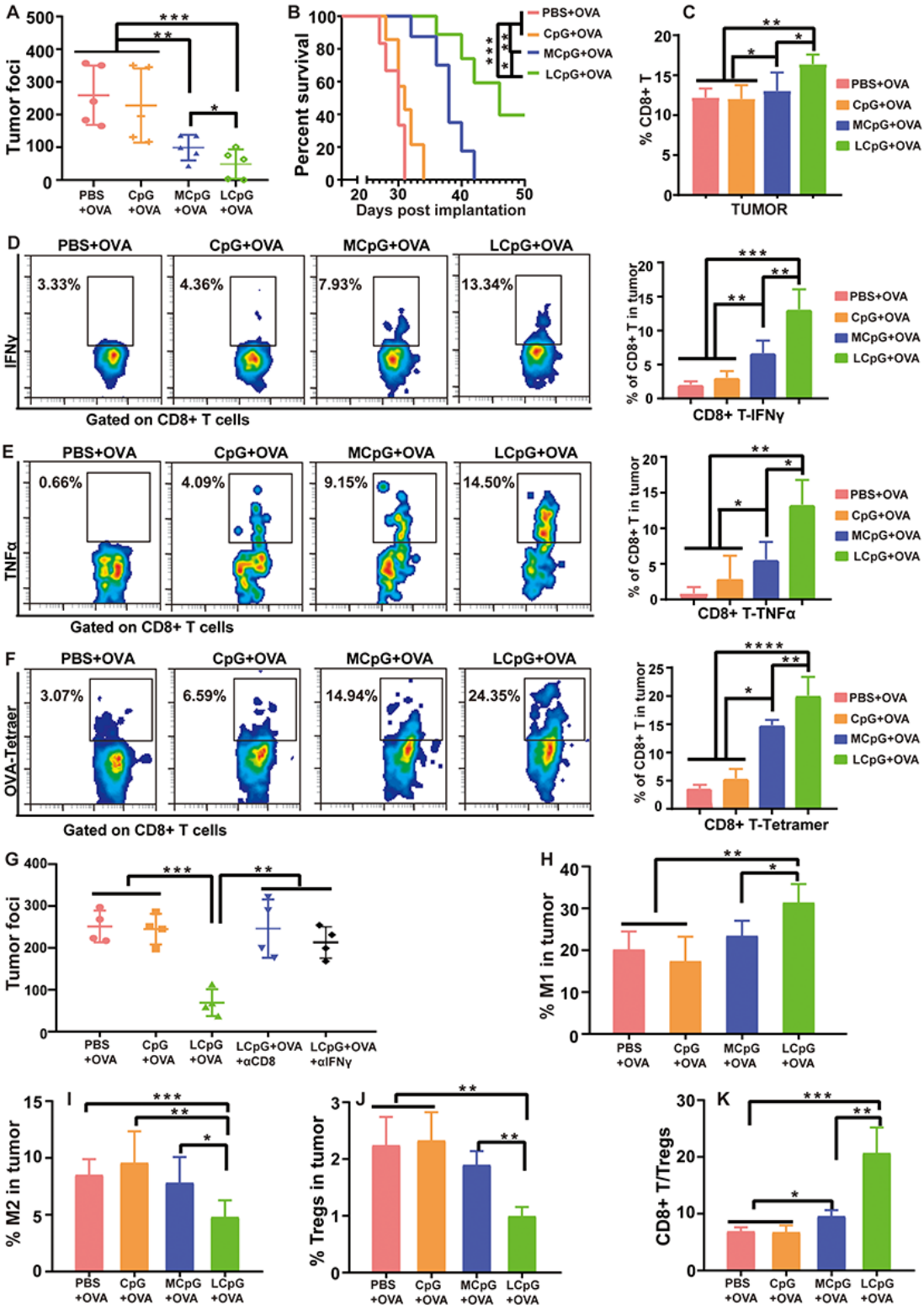

Figure 5

LCpG included vaccine inhibited tumor metastasis by promoting Tc1 and regulating TME. Mice were injected i.v. with 8×105 B16-OVA from tail vein. At day 7 and 12 post tumor inoculation, mice were immunized with different vaccines. Mice were treated with anti-CD8 or anti-IFNγ, on day 6 and repeated every 3 days when indicated. Seven days after the last immunization, mice were sacrificed, and the spleen and TILs from lungs with metastasis were isolated and analyzed by FACs. (A&G) The numbers of

metastatic nodules in the lungs of the tumor-bearing mice. (B) Kaplan-Meier survival of mice were monitored over time. (C) Frequency of CD8+ T in TILs. (D&E) Percentages of IFNγ+ or TNFα+ CD8+ T cells in TILs. (F) Tetramer staining of OVA–specific CD8+ T cells in TILs. (H&I) Frequency of M1 (CD86+ MHCII+) and M2 (CD206+) macrophages. (H) Frequency of Treg in TILs. (I) CD8/Treg ratio. The data shown are the representative of three experiments. *p < 0.05 and **p < 0.01, ***p < 0.001 and ****p < 0.0001.

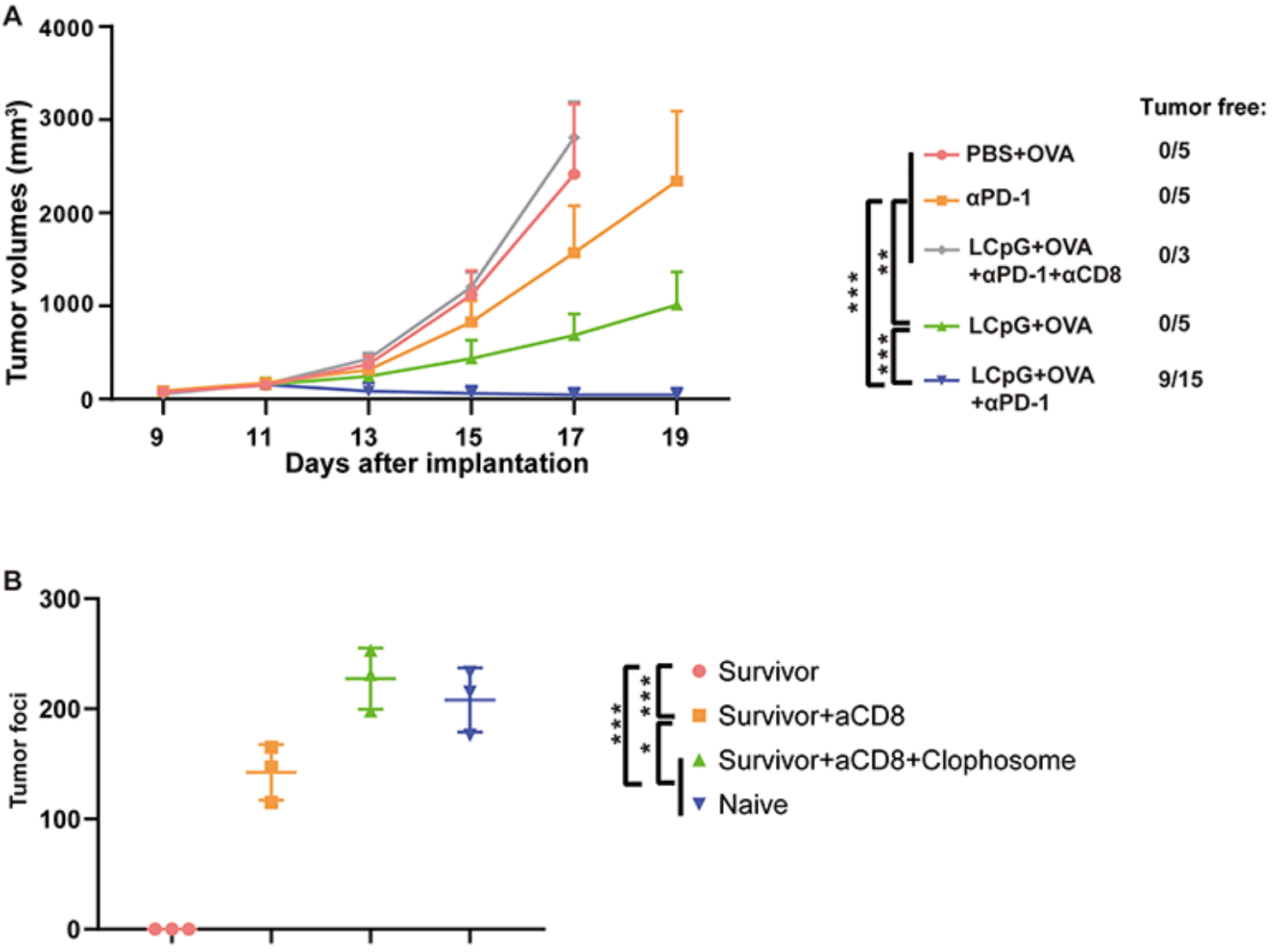

Figure 6

Synergistic effects and memory response induced by LCpG included vaccine combined with anti-PD-1 treatments depends upon CTL. Tumor-bearing mice treated with PBS+OVA, CpG+OVA or LCpG+OVA on day 7 and 12 post tumor inoculation. On days 5 and 10, 200 μg α-PD1 was administered i.p. (A) The tumor volumes were monitored. (B) Survivors and naive mice were i.v. rechallenged with 1.6×106 B16-OVA. Mice were sacrificed and the numbers of metastatic nodules in the lungs were counted 21 days later. The data shown are the representative of three experiments. *p < 0.05 and **p < 0.01, ***p < 0.001 and ****p < 0.0001.

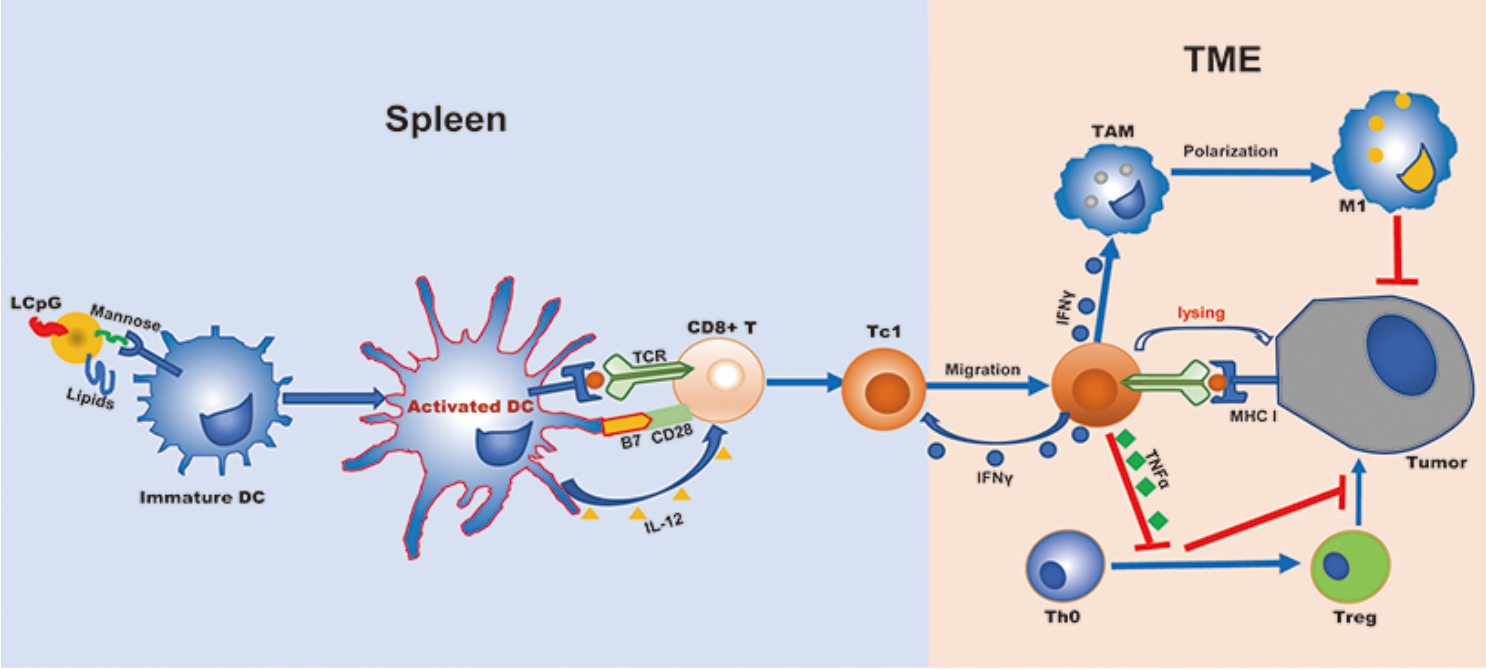

Figure 7

Model of LCpG included vaccine. Tumor-specific T cells are suppressed in TME (scenario 1). LCpG included vaccine promotes DC maturation, activates tumor-specific CTL, increases CTL infiltrating in TME which secretes both IFNγ and TNFα. IFNγ in TME promotes more CTL trafficking into tumor bed, and skews TAM to M1 phenotype. TNFα inhibits Treg differentiation in tumor bed (scenario 2).

Supplementary Files

This is a list of supplementary files associated with this preprint. Click to download.

- SP1.docx